invitrogen

Two data sets. One step. Zero doubt.

Confidently confirm your cell profiles with a new flow cytometer that delivers flow cytometry and imaging data simultaneously. Now, you can acquire dual data quickly and easily. The new Invitrogen™ Attune™ CytPix™ Flow Cytometer delivers both brightfield images and flow cytometry data sets simultaneously, so you can confirm cellular characteristics and sample quality confidently, without changing your protocols.

Enhance analysis and confidence at **thermofisher.com/cytpix**

ThermoFisher SCIENTIFIC

STEM CELLS®

TISSUE-SPECIFIC STEM CELLS

Neutralization of Nerve Growth Factor Impairs Proliferation and Differentiation of Adult Neural Progenitors in the Subventricular Zone

RAFFAELLA SCARDIGLI,[a,b] PAOLO CAPELLI,[c] DOMENICO VIGNONE,[b] ROSSELLA BRANDI,[b] MARCELLO CECI,[b] FEDERICO LA REGINA,[b] ELEONORA PIRAS,[d] SIMONA CINTOLI,[e] NICOLETTA BERARDI,[e,f] SIMONA CAPSONI,[c] ANTONINO CATTANEO[b,c]

Key Words. Nerve growth factor • Adult neurogenesis • Subventricular zone • Neural stem cells • Proliferation • Differentiation

[a]Institute of Translational Pharmacology, National Research Council, Rome, Italy; [b]European Brain Research Institute (EBRI), Rome, Italy; [c]Scuola Normale Superiore, Pisa, Italy; [d]Neuroimmunology Unit, Fondazione Santa Lucia (I.R.C.C.S.), Rome, Italy; [e]Institute of Neuroscience, National Research Council, Pisa, Italy; [f]Department of Neuroscience, Psychology, Drug Research, Child Health NEUROFARBA, Florence University, Florence, Italy

Correspondence: Antonino Cattaneo, PhD, Scuola Normale Superiore, 56126 Pisa, Italy and European Brain Research Institute (EBRI), Via del Fosso di Fiorano 64, 00143 Rome, Italy. Telephone: +39-050509320, +39-06501703118; Fax: +39-06501703335; e-mail: antonino.cattaneo@sns.it

Received September 30, 2013; accepted for publication March 29, 2014; first published online in STEM CELLS *EXPRESS* May 8, 2014.

1066-5099/2014/$30.00/0

http://dx.doi.org/10.1002/stem.1744

ABSTRACT

Adult neurogenesis is a multistep process regulated by several extrinsic factors, including neurotrophins. Among them, little is known about the role of nerve growth factor (NGF) in the neurogenic niches of the mouse. Here we analyzed the biology of adult neural stem cells (NSCs) from the subventricular zone (SVZ) of AD11 anti-NGF transgenic mice, in which the expression of the recombinant antibody aD11 leads to a chronic postnatal neutralization of endogenous NGF. We showed that AD11-NSCs proliferate 10-fold less, with respect to their control counterparts, and display a significant impairment in their ability to differentiate into β-tubulin positive neurons. We found a considerable reduction in the number of SVZ progenitors and neuroblasts also in vivo, which correlates with a lower number of newborn neurons in the olfactory bulbs of AD11 mice and a severe deficit in the ability of these mice to discriminate between different odors. We also demonstrated that, in AD11 mice, the morphology of both SVZ-resident and neurosphere-derived astrocytes is significantly altered. We were able to reproduce the AD11 phenotype in vitro, by acutely treating wild type NSCs with the anti-NGF antibody, further demonstrating that both the proliferation and the differentiation defects are due to the NGF deprivation. Consistently, the proliferative impairment of AD11 progenitors, as well as the atrophic morphology of AD11 astrocytes, can be partly rescued in vitro and in vivo by exogenous NGF addition. Altogether, our results demonstrate a causal link between NGF signaling and proper proliferation and differentiation of neural stem cells from the SVZ. STEM CELLS *2014;32:2516–2528*

INTRODUCTION

Adult neurogenesis is regulated by physiological and pathological processes at different levels, including the proliferation of adult neural stem cells (NSCs), differentiation and fate determination of progenitor cells, and the survival, maturation, and integration of newborn neurons [1]. The two neurogenic niches, the subventricular zone (SVZ) and the subgranular zone of the hippocampal dentate gyrus, have been extensively characterized by different approaches, such as in vivo analysis, in vitro assays, and NSCs transplantation assays [1–4], which allowed the discovery of new markers for the identification and characterization of specific progenitor cell populations. Despite these extensive studies, it is still unclear whether neurogenesis is required for the normal structure and function of the adult brain, and in particular how it is regulated both in physiological and pathological conditions. Multiple growth factors control this important biological process [5]. Among them, some members of the neurotrophins (NTs) family, such as brain-derived nerve factor (BDNF) and neurotrophin-3 (NT-3), together with their corresponding receptors (NTRs) (i.e., TrkB, TrkC, and p75NTR) have been shown to be directly involved in the biology of adult NSCs [6–8]. While NTs are clearly important for the neurogenic process, some controversy remains, regarding their precise effects. Some suggest that NTs promote differentiation, while others suggest that NTs simply promote the survival of the newborn neurons. Regarding nerve growth factor (NGF), very little is known about whether this NT is involved at all in adult neurogenesis. NGF was shown to enhance the in vitro survival and differentiation of NSCs isolated from embryonic forebrain or striatum [9–11], and NGF receptors $p75^{NTR}$ and TrkA have been demonstrated to be involved in the proliferation of embryonic stem cells [12]. Some indirect lines of evidence indicate that NGF and its receptors might regulate progenitor proliferation and/or

differentiation also in adulthood. For instance, in cerebral ischemia animal models, endogenous NGF is upregulated and induces a neuroprotective effect [13], whereas when intranasally delivered it enhances striatal neurogenesis [14]. $p75^{NTR}$ is expressed in mouse and rat adult SVZ progenitors [15], even though its role in regulating their proliferation and differentiation has been studied only in relationship to their responsiveness to BDNF [7, 16]. Altogether, it is not known whether NGF regulates the physiology of adult NSCs in terms of proliferation, maintenance, acquisition of a specific phenotype, and proper differentiation. To address this important issue, we analyzed adult neurogenesis in the AD11 anti-NGF transgenic mice, in which the expression of the recombinant anti-NGF antibody αD11 results in a chronic interference with the activity of endogenous NGF [17].

Materials and Methods

Brain Dissection and Tissue Processing

All experiments with transgenic and control mice were conducted according to national and international laws for laboratory animal welfare and experimentation (EEC council directive 86/609, OJ L 358, 12 December 1987). For NGF nasal delivery, recombinant mouse NGF (450 ng/kg) [18] or Phosphate-buffered saline (PBS) administration was performed on anesthetized 6-month-old AD11 mice as described [19]. Prior to brain dissection, adult mice were anesthetized with about 1 ml of 2,2,2-tribromethanol (Sigma-Aldrich, St. Louis, MO, http://www.sigmaaldrich.com) and intracardially perfused with 4% paraformaldehyde (PFA), whereas newborns were euthanized by decapitation. The whole brain was therefore extracted and the fixation continued in 4% PFA overnight at 4°C for adult mice and 24 hours for newborns. After cryoprotection in 30% sucrose, brains were cryosectioned at 40 μm of thickness, and slices encompassing the SVZ and the olfactory bulbs (OB) were analyzed by immunohistochemistry.

In Vivo Bromodeoxyuridine Labeling

Bromodeoxyuridine (BrdU) was administered to AD11 and control adult mice (6-month-old) at 100 mg/kg by daily intraperitoneal injections for 5 days. Animals were then sacrificed either 7 (for SVZ) or 28 days (for OB) after the last injection, and brains were collected and processed as described before. For postnatal analysis, AD11 and control newborns (P7, P14, and P28) received a single dose of BrdU at 100 mg/kg by intraperitoneal injection and were sacrificed 2 hours after. For NGF rescue experiments, BrdU was administered for 5 days to NGF- or PBS-treated animals, during the last week of the intranasal delivery.

Cell Cultures

NSCs cultures were performed as described [20]. Six-month-old mice (wild-type or AD11) were anesthetized as described before and killed by decapitation. Brains were extracted out of the skull and then located in a brain slicer (Zivic Instrument) in order to obtain coronal slices of 1 mm of thickness. SVZ regions were dissected out of the brain slices by microdissection performed under a stereomicroscope, and cells were isolated by enzymatic digestion (1.33 mg/ml trypsin, 0.7 mg/ml hyaluronidase, and 0.2 mg/ml kynurenic acid) (Sigma-Aldrich) for 30 minutes at 37°C and mechanical dissociation with small-bore Pasteur pipette. Cells were plated at 10^4 cells per cm^2 cells density and cultured in Dulbecco's modified Eagle's medium (DMEM)/F12 medium supplemented with B27 (Invitrogen, San Diego, CA, http://www.invitrogen.com), epidermal growth factor (EGF), and basic fibroblast growth factor (bFGF) (20 and 10 ng/ml, respectively; Peprotech, Rocky Hill, NJ, http://www.peprotech.com) (growing medium) in a humidified incubator at 37°C in 5% CO_2 for 3 weeks. Growth factors were replenished weekly. By the end of 3 weeks, primary neurospheres ($\geq$1 mm in diameter) were subcultured by mechanical dissociation into single cells every 4th day.

Clonal Analysis

Cells isolated from SVZ were cultured under clonal conditions, ensuring that neurospheres are generated from single cells and thus serve as an index of the number of in vivo NSCs [21]. Cells were plated at 5–10 cells per μl (low density) or 50 cells per μl in growing medium. The total number of neurospheres was counted after 3–4 weeks. A minimum of four animals for each genotype was used in three independent set of experiments. Anti-NGF mAb αD11 treatment, to acutely deplete NGF in culture, was performed in freshly isolated wild type (WT) SVZ cells plated at 10 cells per μl in growing medium implemented with 100 ng/ml or 1 μg/ml of purified recombinant αD11 antibody [22]. The antibody was added every day for 7 days, and then the number and size of neurospheres was measured. Mouse IgG was used as control. The size of neurospheres was expressed as a volume calculated after measuring their diameter in phase contrast pictures (assuming a spherical shape). Brightness and contrast images of live neurospheres were taken at a Nikon Eclipse Inverted TE 2000-E microscope, using NIS Elements 3.0 software.

Proliferation Curve and Cell Differentiation

10^4 viable cells at passage 5 were initially plated in a T24 multiwell in growing medium. After 7 days in vitro, the total number of viable cells was counted by Trypan blue exclusion, and all cells were replated under the same conditions at 10^4 per cm^2 cell density. This procedure was repeated for at least four subculture passages, in order to provide the statistical mean of the proliferation index of AD11 versus wild-type progenitors. Where indicated, 100 ng/ml of purified recombinant mouse NGF [18] or BDNF (Peprotech) were added tot the culture every day. The estimated fold increase (total number of cells obtained at a given subculture passage/initial number of seeded cells at the same passage) was then represented using MatLab software.

To assess for differentiation, neurospheres were dissociated into single cells and transferred onto matrigel-coated glass coverslips (12 mm diameter) in differentiating medium (growth medium without EGF and FGF) at 5×10^4 cells density. Five days after plating, cultures were fixed in 4% PFA and processed for immunocytochemistry. For NGF treatment, purified recombinant mouse NGF [18] was added at 50 ng/ml to proliferating progenitors every day for 5 days and then to the differentiating cells every day for 5 days. Where differently indicated, NGF was added only during differentiation. For anti-NGF treatment, 100 ng/ml of mAb αD11 was added to the proliferating progenitors every day for 5 days and then

cells were induced to differentiate as described, in the presence of the anti-NGF antibody (every day for 5 days). As control, mouse IgG was used at the same concentration. Where differently indicated, mAb αD11 was added either during proliferation or differentiation. For co-cultures experiments, primary hippocampal neurons were prepared as described [23]. 8×10^4 primary neurons were cultured for 1 week on polylysine-coated coverslips (12 mm), and then dissociated neurospheres were added to the neuronal cultures at 5×10^4 cell density per coverslip in differentiating medium and let differentiate for the following 5 days.

Immunocytochemistry on Brain Sections and Neurospheres

Immunohistochemistry of SVZ and OB was performed on 40-μm serial free-floating sections. To improve the efficiency of BrdU detection, the sections, prior to antibody staining, were exposed to 2 N HCl for 45 minutes at 37°C and then washed with 0.1 M sodium borate buffer pH 8.5 for 10 minutes (to allow the denaturation of DNA, necessary to expose the BrdU). Immunostaining on cell cultures was performed after fixation in 4% PFA for 10 minutes at room temperature. Neurospheres were plated on matrigel-coated coverslips 2 hours before the fixation. Upon fixation, sections or cells were permeabilized in 0.3% or 0.1% Triton X-100, respectively, in PBS and then incubated with the antibody of interests, as described in Supporting Information Materials. The total number of cells in each field was determined by counterstaining cell nuclei with 4,6-diamidine-2-phenylindole dihydrochloride (DAPI; Sigma-Aldrich; 50 mg/ml in PBS for 15 minutes at RT). Immunostained sections and cells were mounted in Aqua-Poly/Mount (Polysciences, Inc., Warrington, PA, http://www.polysciences.com) and analyzed at fluorescent or confocal microscopy, using a Nikon Eclipse 90i microscope (Nikon) or a TCS SP5 microscope (Leica Microsystem). Z-stacks images were captured at 1 μm intervals with a ×40 or ×60 objectives and a pinhole of 1.0 Airy unit. Analyses were performed in sequential scanning mode to rule out cross-bleeding between channels. Fluorescence intensity quantification was performed with ImageJ software.

Quantification of Cell Numbers

Stereological analysis of the number of cells was performed on series of 40-μm free-floating coronal sections comprising the entire SZV or OB, which were analyzed by confocal microscopy to count cells expressing BrdU throughout the whole rostro-caudal extent of these structures, counting three regions per section (top, central, and bottom). To obtain the average number of SVZ or OB cells per square millimeter, the number of positive cells for each SVZ and OB section was multiplied by the total number of sections encompassing the entire structure. Three animals per group ($n = 3$) were analyzed. Statistical analysis was performed by unpaired Student's *t* test, and all experiments were expressed as mean ± SEM.

To quantify the number of differentiated cells, the number of Tuj1, glial fibrillary acid protein (GFAP), and O4 immunoreactive cells was counted in at least 10 nonoverlapping fields in each sample, for a total of >1,000 cells per sample. The total number of cells in each field was determined by counterstaining cell nuclei with DAPI (Sigma). The average percentage of differentiated cells for each samples was then calculated by dividing the number of Tuj1, GFAP, and O4 positive cells by the total number of cells for each fields. Data are the mean ±SEM of three independent cultures ($n = 3$), three independent experiments for each culture. Statistical analysis was performed by unpaired Student's *t* test.

RNA Isolation and Reverse Transcription-Polymerase Chain Reaction

RNA was isolated from three different AD11 and three different WT neurosphere cultures. Briefly, neurospheres were lysed with Trizol (Invitrogen) and DNAse treated by Qiagen columns. RNA quantity was determined on a NanoDrop UV-VIS. Only samples with an absorbance ratio of 1.8,OD260/OD280,2.0 were processed further. Each sample was then quality checked for integrity using the Agilent BioAnalyzer 2100 (Agilent G2938C, RNA 6000 nano kit; Agilent, Santa Clara, CA, http://www.agilent.com): samples with a RNA Integrity Number index lower than 8.0 were discarded. The purified RNA was used for quantitative reverse transcriptase polymerase chain reaction (qRT-PCR). The first strand cDNA template was synthesized from 500 ng of total RNA using random primers and Superscript III reverse transcriptase (Invitrogen). All reactions were performed with SYBR Green PCR Master Mix (Bio-Rad, Hercules, CA, http://www.bio-rad.com) and carried out in the iCycler (Bio-Rad). Primers for quantitative PCR (QTR-PCR) analysis were designed with the assistance of Universal Probe Library Software (Roche Applied Science, Basel, Switzerland, http://www.roche-applied-science.com) and are described in Supporting Information Materials. All samples were analyzed in triplicates. Relative change of mRNA amount was calculated based DCt method, as described [24].

Protein Extraction from Neurospheres and Western Blotting

Homogeneous suspension of growing neurospheres (about 25 ml of growing medium from a 75 cm^2 flask) was lysed in 50 mM Tris HCl pH 7.4, 150 mM NaCl, 1 mM EDTA, 0.05% Triton plus proteases inhibitors (Complete Protease Inhibitor Cocktail, Roche) for 30 minutes in ice. As positive control for activated caspase-3 detection, cells were treated with 0.5 μM staurosporine (Life Technologies, Grand Island, NY, http://www.lifetech.com) for 4 hours prior to protein extraction. For phosphorylated AKT and total AKT detection, cells were starved overnight in DMEM/F12 and then challenged with 100 ng/ml of purified recombinant mouse NGF [18] for 30 minutes at 37°C, prior to protein extraction. 50–100 μg of proteins was loaded on SDS-PAGE 10% and Western blotting was performed as described [23]. The following primary antibodies were used: rabbit polyclonal anti-phosporylated-AKT (Cell Signaling Technology, Beverly, MA, http://www.cellsignal.com, 9271, 1:1,000); rabbit polyclonal anti-total AKT (Cell Signaling Technology, 9271, 1:1000); rabbit polyclonal anti-activated Caspase-3 (cleaved caspase-3, Cell Signalling Technology, 9664, 1:1,000); mouse anti-β-actin (Sigma-Aldrich, A5316, 1:10,000); rabbit polyclonal anti-Musashi 1 (Msi1, Merck Millipore, Germany, http://www.millipore.com; AB5977, 1:1,000); mouse anti-Sox2 (Merck Millipore; 6F1.2, 1:500). Secondary horseradish peroxidase-conjugated anti-mouse or anti-rabbit antibodies and ECL reagent (GE Healthcare, Fairfield, CT, https://www.ge.com/) were used. Chemiluminescence's signal was analyzed by Kodak Image Station 2000R and quantified with the Kodak Molecular Imaging Software, as a measure of the protein expression level.

Results

SVZ Progenitors of Adult Anti-NGF AD11 Mice Show a Proliferative Impairment

In order to study the influence of NGF on adult neurogenesis, NSC were isolated from the SVZ region of 6-month-old anti-NGF AD11 mice and grown as neurosphere cultures [25]. In AD11 mice, the bioactivity of endogenous NGF is neutralized in the adult brain by the expression of the αD11 anti-NGF antibody transgene [17, 26] that selectively binds mature NGF with a picomolar affinity [18]. Therefore, we first verified whether resident (in vivo) and SVZ-derived (in vitro) neural progenitors express the anti-NGF antibody αD11. A double immunostaining for the human heavy and light chains of the transgenic antibody was performed on SVZ sections and on bulk neurospheres obtained from different AD11 and control animals. We could detect the presence of the recombinant anti-NGF, as shown by the concomitant immunoreactivity for the two antibody chains [17], in the SVZ region of AD11 mice (green and red signals in upper panels, respectively, of Fig. 1A), and not, as expected, of control mice. Interestingly, the anti-NGF antibody expression persists in vitro, as demonstrated by the double immunostaining for the two antibody chains also in the AD11 neurospheres and not in the WT ones (Fig. 1B, upper and lower panels, respectively). These expression data were further confirmed by real-time PCR for the heavy and light chains mRNA (Fig. 1C). The expression of the recombinant mAb αD11 is not expected to provoke a decreased synthesis of NGF but only a neutralization of NGF activity, as a ligand scavenger. Consistently, immunofluorescence for NGF demonstrates that endogenous NGF is also expressed in the AD11 neurospheres as well as in the WT counterpart (Fig. 3A, left panel). The overall number of primary neurospheres obtained by individual SVZ dissections from AD11 mice was significantly lower than from WT animals (Fig. 2A). Moreover, the majority of AD11 neurospheres were smaller in size, compared to their control counterpart ($\leq$50 μm of diameter, 68% in AD11, 21% in WT, Fig. 2B; Supporting Information Fig. 1A) and expressed lower levels of NSC and progenitor markers, such as Musashi1 (Msi1) and Sox2, as shown by immunofluorescence and by Western blot analysis on bulk neurospheres (Fig. 2E, 2F). These data could reflect either a proliferative impairment of the SVZ progenitors and/or reduction in the number of NSC resident in the SVZ. To address this point we performed growth curves of progenitors at early passages. Figure 2C shows that AD11 NSCs proliferated significantly much less than WT progenitors, with an average 10-fold difference. This result was confirmed by measuring the expression of the pan-proliferative marker Ki67 and BrdU incorporation after short (30 minutes) in vitro BrdU labeling. Double immunostaining for Ki67 and BrdU 48 hours after BrdU pulse showed that the percentage of proliferating Ki67+ and Ki67/BrdU positive cells was significantly lower in AD11 respect to WT, while the percentage of quiescent/resting cells (Brdu+/Ki67−) increased (Supporting Information Fig. 1C), suggesting a delayed cell cycle rate of AD11 cells. Indeed, cell cycle analysis showed an increase in the G0-G1 phase and a reduction in the G2/M phase of AD11 respect to WT cells (Supporting Information Fig. 1D, 1E). The proliferative impairment of AD11 progenitors is not due to an increase in apoptosis, as there are no difference in the sub-G1 phase of the two populations (not shown) and the activated form of caspase 3 is detectable at very low levels in both WT and AD11 neurospheres extracts (Fig. 2D). To further confirm that this defect is indeed due to NGF neutralization, we repeated the clonogenic assay with WT progenitors in the presence of anti-NGF αD11 antibody. As shown in Figure 2G, the addition of 100 ng/ml or 1 μg/ml of αD11 significantly reduced the number of primary neurospheres by about 25% and 50%, respectively, in a dose-dependent manner, with respect to the control (mouse IgG). This is due to a lower proliferation of anti-NGF-treated progenitors, as demonstrated by the smaller size of the corresponding neurospheres ($\leq$50 μm of diameter, 72% in AD11, 16% in WT, Fig. 2H; Supporting Information Fig 1B).

Increased Proliferation of AD11 Progenitors in Response to Exogenous NGF

The proliferative impairment of AD11-SVZ progenitors is likely to be due to NGF neutralization occurring at an adult stage. In this view, we asked if these cells still retain the ability to respond to NGF, and thus if their phenotype could be rescued by an in vitro exposure to NGF. We first verified by immunofluorescence the expression of NTRs p75 and TrkA in both WT and AD11 bulk neurospheres. AD11 progenitors express NGF, as mentioned before, as well as p75 and TrkA receptors, at levels comparable to those of WT cells (Fig. 3A). We then performed growth curves as described above, in the absence or presence of 100 ng/ml of NGF or BDNF, a NT widely accepted to be involved in NSCs proliferation [7, 16]. As shown in Figure 3B, when NGF was added to the cultures, AD11 progenitors significantly increased their proliferative rate (about two and six times more in AD9912 and AD9883 clones, respectively), with respect to the untreated (ct) or BDNF-treated samples, whereas the proliferation of NGF-treated WT cells was similar to that of untreated and BDNF-treated counterparts. Interestingly, the different proliferative response of the two AD11-derived cultures, after challenge with exogenous NGF, correlates well with the different level of NGF signaling activation, in the two cultures, as shown by the increased amount of the phosphorylated-AKT protein upon NGF stimulation in vitro for 30 minutes (Fig. 3C, 3D). This is not due to an overall increase of AKT expression, as levels of total AKT protein remain unchanged between control and treated cells.

Reduced Proliferation and Maturation of SVZ Progenitors in AD11 Mice In Vivo

The proliferative impairment of AD11 neurospheres observed in vitro could reflect an intrinsic proliferative feature of the adult NSCs cells from AD11 mice in vivo, and for this reason we measured proliferation of AD11 SVZ progenitors in vivo by BrdU labeling experiments. Adult transgenic and control mice (6-month-old) received daily BrdU intraperitoneal injections (100 mg/kg) for 5 days and were sacrificed 1 week from the first injection for the analysis of BrdU expression in the SVZ. The control mice showed BrdU positive cells all along the wall of the ventricle (Fig. 4A). In contrast, AD11 mice present a marked decrease in the number of cells in proliferation (Fig. 4A and quantification in 4B). As consequence of this proliferative impairment, the thickness of the lateral ventricle walls corresponding to SVZ was greatly reduced in 6-month-old AD11 compared to control mice (Fig. 4A, bottom panels).

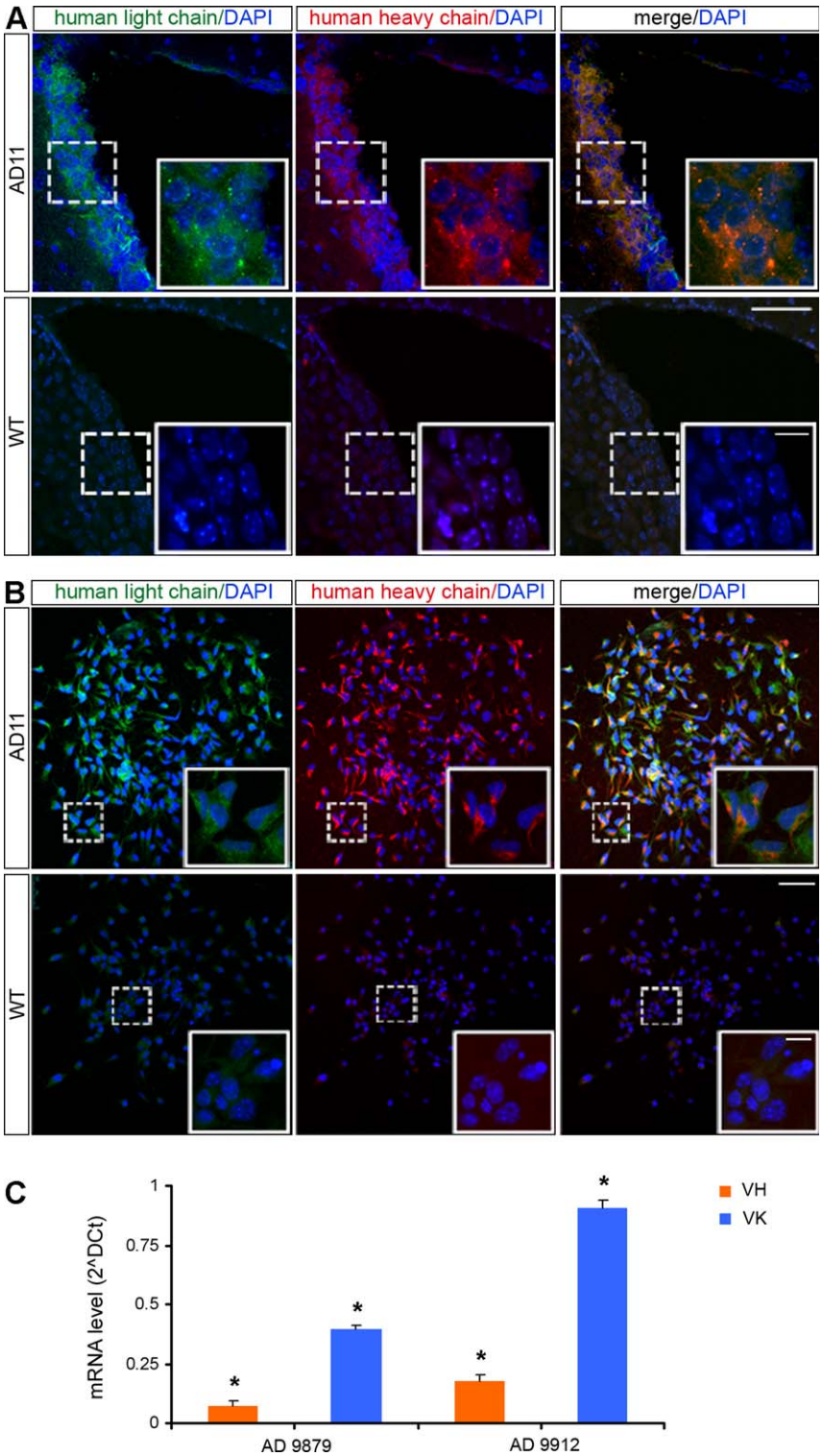

Figure 1. Expression of recombinant αD11 antibody in AD11 subventricular zone (SVZ) region and SVZ-derived neurospheres culture. **(A, B):** Immunofluorescence staining for the light (kappa chain, green) and heavy chain (γ chain, red) of mAb anti-nerve growth factor (αD11) showing that the antibody is expressed both in the SVZ region and in SVZ-derived neurospheres cultures of AD11 mice (A and B, upper panels) but not in those of WT animals (A and B, lower panels). White boxes in each panel represent ×63 magnification of the corresponding dot-lines insets. DAPI staining on nuclei in blue. Scale bars = 50 and 10 μm (enlargements). **(C):** Real-time polymerase chain reaction for messenger RNA of heavy chain (VH) and light chain (VK) confirms the expression of αD11 antibody in two independent AD11 clones ($n = 2$). Data are means ± SEM of two independent experiments. *, $p < .05$, significantly different from WT; Student's t test. Abbreviations: DAPI, 4,6-diamidine-2-phenylindole dihydrochloride; VH, heavy chain; VK, light chain; WT, wild type.

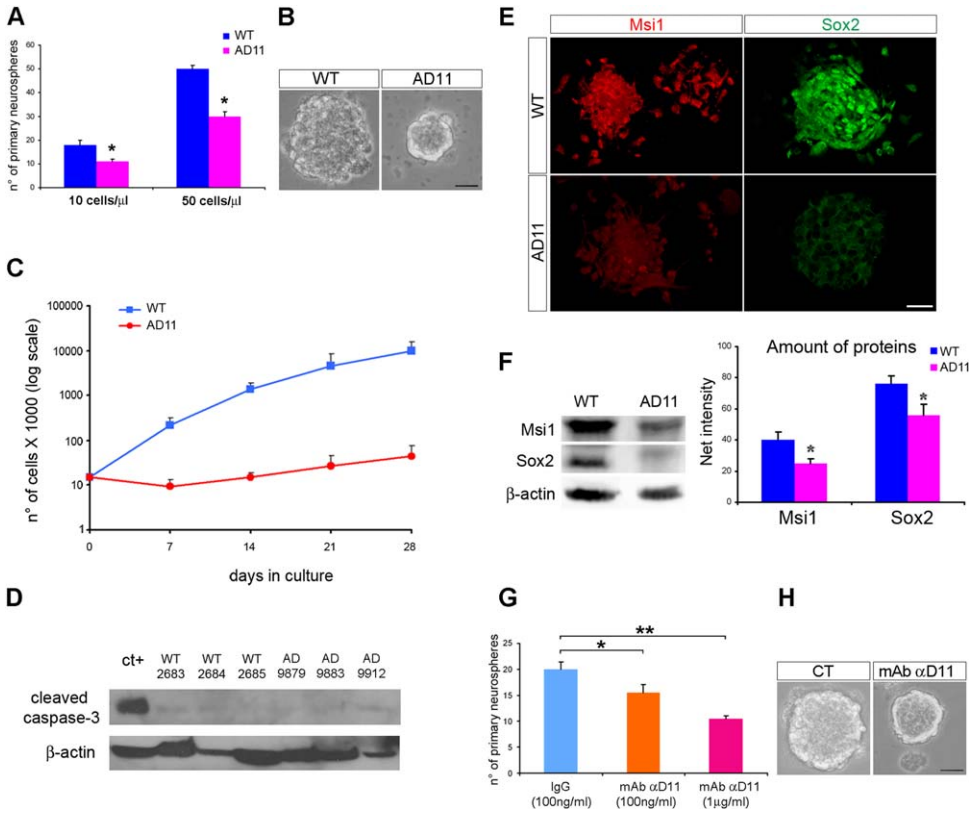

Figure 2. Subventricular zone (SVZ) progenitors' proliferation is affected in AD11 mice. **(A):** Number of primary neurospheres obtained from WT- and AD11-SVZ progenitors, plated at low (10 cells per μl) or high (50 cells per μl) cellular density. AD11 cells give rise to less neurospheres in vitro, compared to WT animals. Data are means ± SEM of four individual animals ($n = 4$) for each genotype. *, $p < .05$, significantly different from WT; Student's t test. **(B):** Phase-contrast micrograph of neural stem cells (NSCs) culture showing that AD11 neurospheres (right panel) are smaller in size than WT counterparts (left panel). Scale bar = 25 μm. **(C):** Proliferative rate of WT and AD11 neurospheres derived from single animal SVZ, at different passages. AD11 NSCs proliferate significantly less than their WT counterparts ($n = 3$ for each genotypes). **(D):** Western blot analysis for cleaved caspase-3 (upper panel) and β-actin (lower panel) in three different WT and three AD11 neurosphere cultures ($n = 3$), showing no difference in apoptosis between the two genotype populations. ct+: staurosporine-treated neurosphere extract. **(E, F):** Progenitor markers are significantly reduced in SVZ-derived neurospheres. (E): Immunofluorescence staining for Msi1 (red) and Sox2 (green) in bulk neurospheres shows that AD11 SVZ (bottom panels) contains less NSCs than control animals (upper panels). (F): Representative Western-blot analysis for Msi1 and Sox2 proteins in WT and AD11 neurospheres (left panel) and protein quantification of Msi1 and Sox2 expression (right panel), as mean ± SEM of three independent experiments ($n = 3$).*, $p < .05$, significantly different from WT, Student's t test. **(G):** Clonal analysis of WT progenitors in the presence of anti-nerve growth factor mAb αD11 antibody. Number of primary neurospheres obtained from WT SVZ progenitors plated at low cellular density (10 cells per μl) and treated for 1 week with control IgG antibodies (100 ng/ml, light blue bar) or mAb αD11 antibody (100 ng/ml, orange bar, and 1 μg/ml, red bar). Neurosphere numbers are represented as mean ± SEM of three independent experiments. *, $p < .05$; **, $p < .01$, significantly different from WT, Student's t test. mAb αD11-treated progenitors give rise to less primary neurospheres, in a dose-dependent manner, which are also smaller in size respect to the control (H, left and right panels, respectively). Scale bar = 25 μm. Abbreviations: Msi1, Musashi 1; WT, wild type.

Since αD11 antibody is transiently expressed at embryonic stage E13 [27], we wanted to exclude that the proliferative impairment of AD11 progenitors might be a developmental consequence of a transient early neutralization of NGF. To this aim, BrdU labeling experiments were performed in AD11 newborns, with a single pulse of BrdU (see Materials and Methods for details), at postnatal stages P7 and p14 when the transgenic antibody is not expressed yet, or at P28 when αD11 mRNA starts to be expressed [27, 28]. As shown in Figure 4C, no significant difference was observed, between AD11 and control newborns, in the number of SVZ-BrdU positive cells at early postnatal stages (P7 and P14), whereas AD11 animals start showing a decrease in the SVZ progenitor proliferation at P28. These results, together with the data presented above, demonstrate that the phenotype of AD11 progenitors is due to the NGF neutralization occurring at adult stage. To further confirm this conclusion, we tried to rescue this phenotype by the intranasal delivery of NGF in AD11 animals, which has been reported to rescues recognition memory deficits in AD11 mice [29]. As shown in Figure 4D, 4E, the delivery in vivo of NGF to AD11 mice increased the number of BrdU+ cells, compared to control, PBS-treated animals, indicating that the proliferative impairment of AD11-SVZ progenitors can be partly rescued by the addition of exogenous NGF, as we shown in vitro.

The reduced size of the SVZ in AD11 animals correlates with a lower number of resident progenitors and neuroblasts, as demonstrated by the expression levels of the NSC and progenitor markers Msi1, Sox2, Pax6, and Doublecortin (Dcx) [30]. Indeed, the immunofluorescence staining performed on coronal brain sections encompassing the SVZ area showed a significant reduction in the expression level

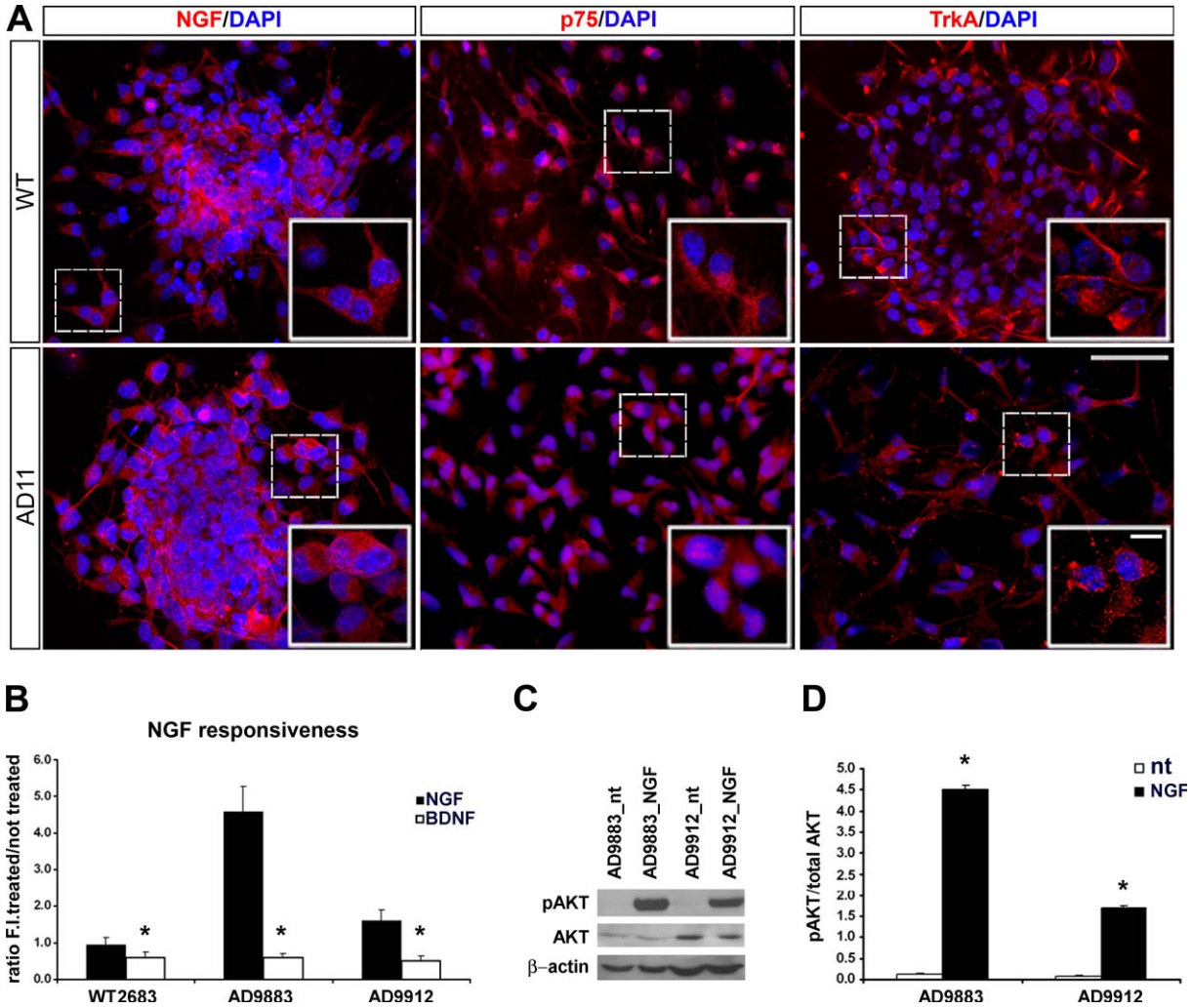

Figure 3. Responsiveness to NGF of AD11 progenitors. **(A):** Immunostaining for NGF, p75, and TrkA (red signal in left, central and right panels, respectively) in neurospheres derived from WT (upper) and AD11 (bottom) mice. Both WT and AD11 neural stem cells (NSCs) express NGF and its relative receptors in vitro. White square boxes in each panel represent ×63 magnification of the corresponding dot-lines insets. Scale bars = 50 and 10 μm (enlargements). **(B):** AD11 progenitors' proliferation increases in response to exogenous NGF. Two different AD11 progenitor populations ($n = 2$) show a higher fold increase than WT cells when treated with NGF to respect to the control or BDNF-treated counterparts, as mean ± SEM of three independent experiments. **(C, D):** Differential pAKT signaling induction by short pulse of NGF in the same AD11 progenitors populations correlates with their different response to NGF. (C): Western blot analysis for pAKT, total AKT, and β-actin showing more NGF-induced phosphorylated AKT protein in AD9883 cells than in AD9912. (D): Protein quantification of pAKT by densitometry of Western blot in panel (B), expressed as pAKT/total AKT ratio, as mean ± SEM of three independent experiments. *, $p < .05$, significantly different from WT, Student's t test. Abbreviations: BDNF, brain-derived nerve factor; DAPI, 4,6-diamidine-2-phenylindole dihydrochloride; F.I., fold increase; NGF, nerve growth factor; pAKT, phosphorylated AKT; WT, wild type.

of these markers in AD11 mice, compared to WT animals (Fig. 4F).

In order to better identify the possible cellular targets of the NGF neutralizing action of the antibody, we investigated the presence of NGF in the SVZ. Since the NGF mRNA is expressed at low levels in this region (Supporting Information Table I), we performed our analysis on single cells dissected out from the SVZ and kept in culture for 24 hours (see Materials and Methods section). Both nestin+/GFAP+/Sox2+ progenitors and some Dcx+ neuroblasts express NGF protein at levels comparable to those present in β-tubulin+ differentiated neurons (Supporting Information Fig. 2A, 2B), as well as p75 and TrkA receptors (Supporting Information Fig. 2C). Thus, it is likely that the action of anti-NGF antibodies is directed to both progenitors and neuroblasts, and that the reduction of these populations in the SVZ niche is a direct consequence of the neutralization of the endogenous NGF, which might be part of a paracrine or an autocrine loop, also involving p75 and TrkA receptors.

OB Neurogenesis Is Reduced in AD11 Mice

As OBs neurogenesis is sustained by the NSCs resident in the SVZ, we measured the number of newborn neurons in the OBs of AD11 mice, by in vivo BrdU labeling experiments. Four weeks after a 5-day pulse of BrdU, animals were sacrificed and the OBs were analyzed for the concomitant expression of BrdU and the mature neuronal marker NeuN. In accordance with the neurogenic defects of SVZ progenitors, AD11 mice display a significant loss of newborn OB neurons, as shown in Figure 5A and 5C, whereas the total number of NeuN+ cells

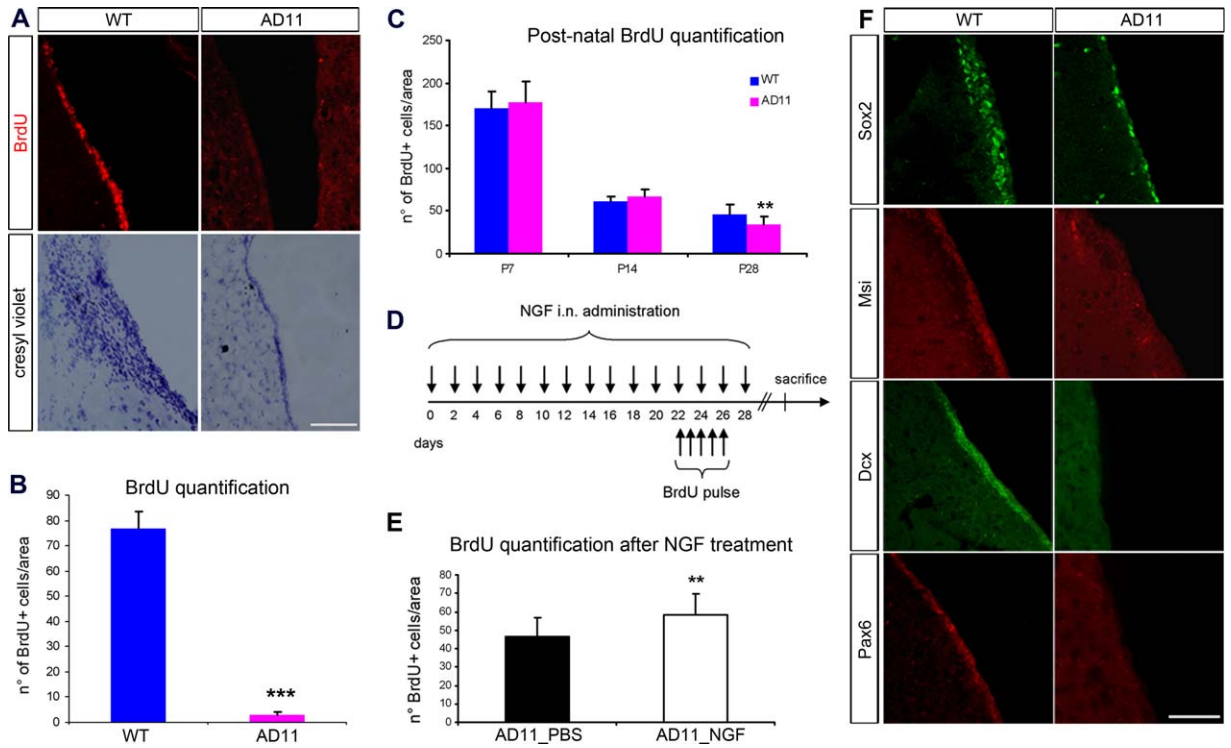

Figure 4. In vivo proliferation of subventricular zone (SVZ) progenitors is affected in AD11 mice. **(A):** Immunostaining for BrdU (red) incorporated in stem cells and progenitors shows a decrease in cell proliferation in AD11 SVZ (upper right panel), compared to WT (upper left panel). As consequence, the SVZ of AD11 mice is significantly reduced in thickness, as shown by the cresyl-violet staining on lateral ventricles from AD11 (bottom right panel) and control (upper left panel). **(B):** Quantification of BrdU positive cells in 6-month-old AD11 (magenta) and control (blue) mice. (**C**): Postnatal analysis of SVZ progenitor proliferation from WT and AD11 newborns at different ages (P7, P14, and P28) by BrdU in vivo labeling. While the number of BrdU+ cells do not vary significantly between WT and AD11 young newborns (P7 and P14), we observed a decrease of BrdU+ cells in AD11 p28 mice, when the transgenic antibody begins to be expressed. **(D, E):** The intranasal delivery of NGF partly rescues AD11 progenitors' proliferation. (E): In vivo BrdU labeling, performed as described in the timeline (D), shows an increase of about 20% in the number of BrdU+ SVZ cells after NGF treatment (white bar), compared to control. PBS-treated animals (black bar). (**F**): Immunofluorescence staining for stem cell (Msi1 and Sox2) and neuroblast markers (Dcx, Pax6) showing significant reduction in the NSCs compartment in AD11 SVZ. Cell numbers in the SVZ in B, C, and E were measured as described in Materials and Methods section and are represented as mean ± SEM of the analysis of three animals per group. **, $p < .01$; ***, $p < .001$, significantly different from WT, Student's *t* test. Scale bars = 100 μm. Abbreviations: BrdU, bromodeoxyuridine; Dcx, Doublecortin; Msi, Musashi; NGF, nerve growth factor; PBS, Phospate-buffered saline; WT, wild type.

remains equal between the two populations (Fig. 5B), probably due to the decreased neuronal turnover in the olfactory system of aged (6–12 months old) mice, as described [31].

We thus investigated if this neurogenic defect in the OB led to alterations in their odor discrimination ability. To this aim, we performed a social transmission of food preference test [32], in a format in which it provides a measure of the capacity to discriminate odors and not cognitive deficits, since the interval between the interaction with the demonstrator and the test for odor preference is too brief to account for memory deficits [33] (see Materials and Methods section). A greater percentage of WT observer mice ate more cocoa-flavored than cumin-flavored food (Fig. 5D). On the contrary, while the number of sniff interactions was similar between the two groups (Fig. 5E), AD11 observer mice showed no significant difference for preference of the cued food (Fig. 5C), demonstrating, indeed, an alteration in their olfactory ability and odor discrimination.

Impaired Differentiation of AD11 NSCs

In addition to the proliferative defect of SVZ progenitors, an impairment of their differentiation into olfactory interneurons could also participate in generating the OB phenotype. To address this point, we tested the differentiating potential of AD11 neural progenitors in vitro, by measuring the expression of the neuron-specific class III β-tubulin (TuJ1), upon neurospheres dissociation and differentiation on matrigel-coated coverslips (see Materials and Methods section). Tuj1 immunostaining of differentiated neurospheres showed that AD11 progenitors have an impaired ability to differentiate into neuronal cells (red signal in Fig. 6A) with respect to their WT counterpart. This was confirmed in different AD11 independent clones and quantified by counting the percentage TuJ1+ cells over the total of DAPI positive nuclei (Supporting Information Fig. 3A, see Materials and Methods section for details). Consistently, AD11 progenitors expressed low levels of Ngn2 (Supporting Information Fig. 3B), which is known to be one of the leading proneural gene involved in neurogenesis [34]. In the same real-time PCR experiment we also demonstrated that β-tubulin mRNA was downregulated (Supporting Information Fig. 3C), confirming the expression data reported in Figure 6A.

In vitro differentiation of AD11 neurospheres revealed an unbalance in the relative pools of glial subtypes:

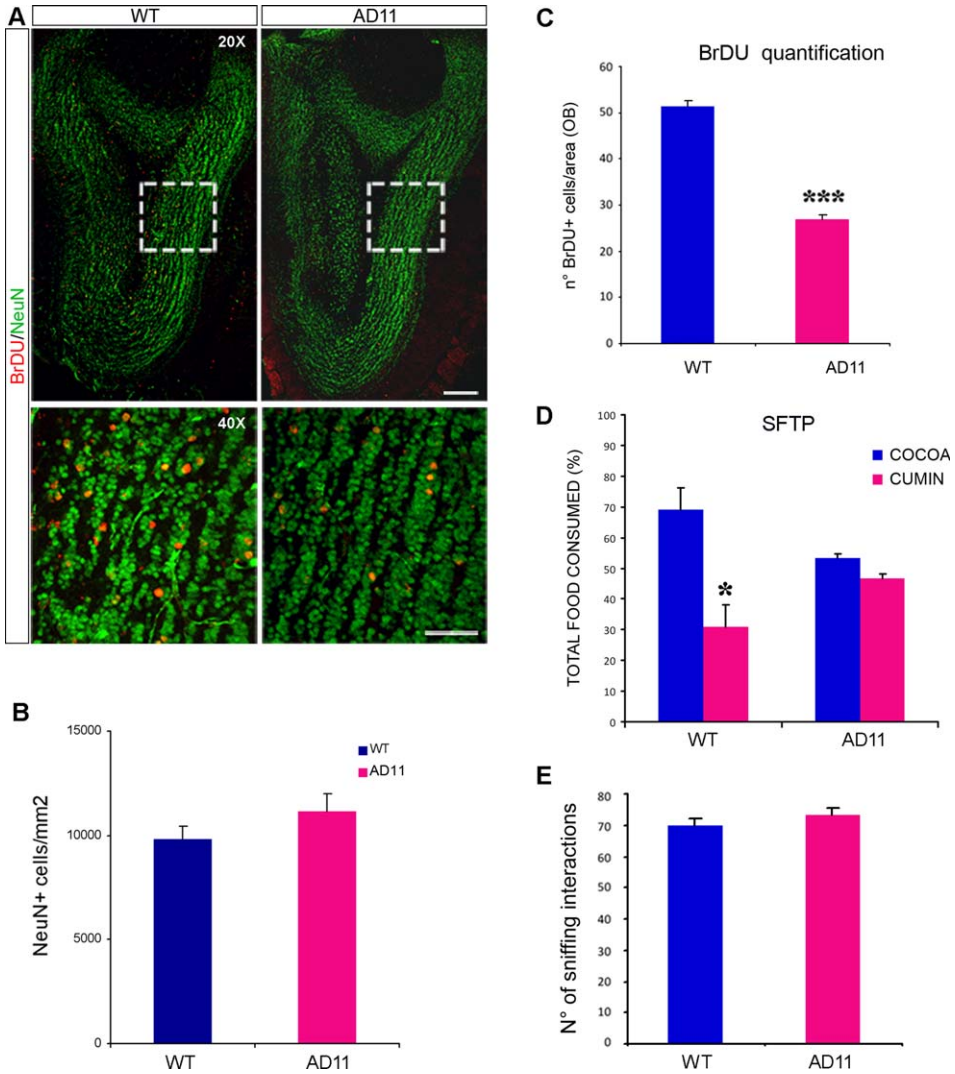

Figure 5. Olfactory bulb neurogenesis is reduced in AD11 mice. **(A):** BrdU/NeuN double labeling in WT (left panel) and AD11 (right panel) adult mice revealed less newborn neurons in AD11 olfactory bulbs. Square panels represent ×40 magnification of insets in AD11 and WT, respectively. **(B, C):** Quantification of total NeuN+ cells (B) and of total BrdU+/NeuN+ cells (C) in WT and AD11 OBs. Cell numbers in OB were measured as described in Materials and Methods section and are represented as mean ± SEM of the analysis of three animals per group. ***, $p < .001$, significantly different from WT, Student's t test. Scale bars = 50 and 100 μm (enlargements). **(D, E):** Alterations in olfactory ability and odors discrimination in AD11 mice. Amount of cocoa and cumin flavoured diet, as a percentage of total intake, eaten by 7-month-old WT and AD11 mice. WT observer mice ate significantly more of the cocoa-flavored diet cued food than cumin-flavored food (two way RM ANOVA, post hoc analysis Holm-Sidak method, *, $p = .020$), indicating an impairment of AD11 mice in odor discrimination. This defect is not due to a reduced number of sniff interactions between tester and observer mice, as reported in histogram in (E). Abbreviations: BrdU, bromodeoxyuridine; OB, olfactory bulb; STFP, social transmission of food preference; WT, wild type.

GFAP expressing cells were significantly reduced in number, while O4+ oligodendrocytes increased compared to WT (Fig. 6A; Supporting Information Fig. 3A). Interestingly, GFAP+ cells, differentiated from AD11 progenitors, lost the bushy-like morphology, typical of astrocytes, and displayed an elongated shape with few ramifications (Fig. 6A, compare magnifications between right panels), as also confirmed by the expression pattern of another astrocytic marker, S100 beta (S100b) (Fig. 6B). This phenotype did not depend on the reduced number of differentiated neurons from AD11 neurospheres, as the same altered GFAP+ astrocytes were obtained in cocultures of AD11 progenitors with WT primary neurons (Supporting Information Fig. 4). Moreover, the AD11 astrocytes phenotype was present also in vivo, in the SVZ region, where GFAP+ cells display the same atypical elongated shape observed in their in vitro counterpart (Fig. 6C). These data strongly suggest that the glial defect observed in the differentiated neurospheres cultures is due to an intrinsic defect of the astrocytes progenitors, caused by the chronic neutralization of NGF occurring in vivo in AD11 animals. To test this hypothesis, we verified whether WT neurospheres, never exposed to anti NGF antibodies in vivo, were sensitive to acute NGF deprivation, after having been placed in culture. Interestingly, upon mAb αD11 treatment of WT progenitors, GFAP+

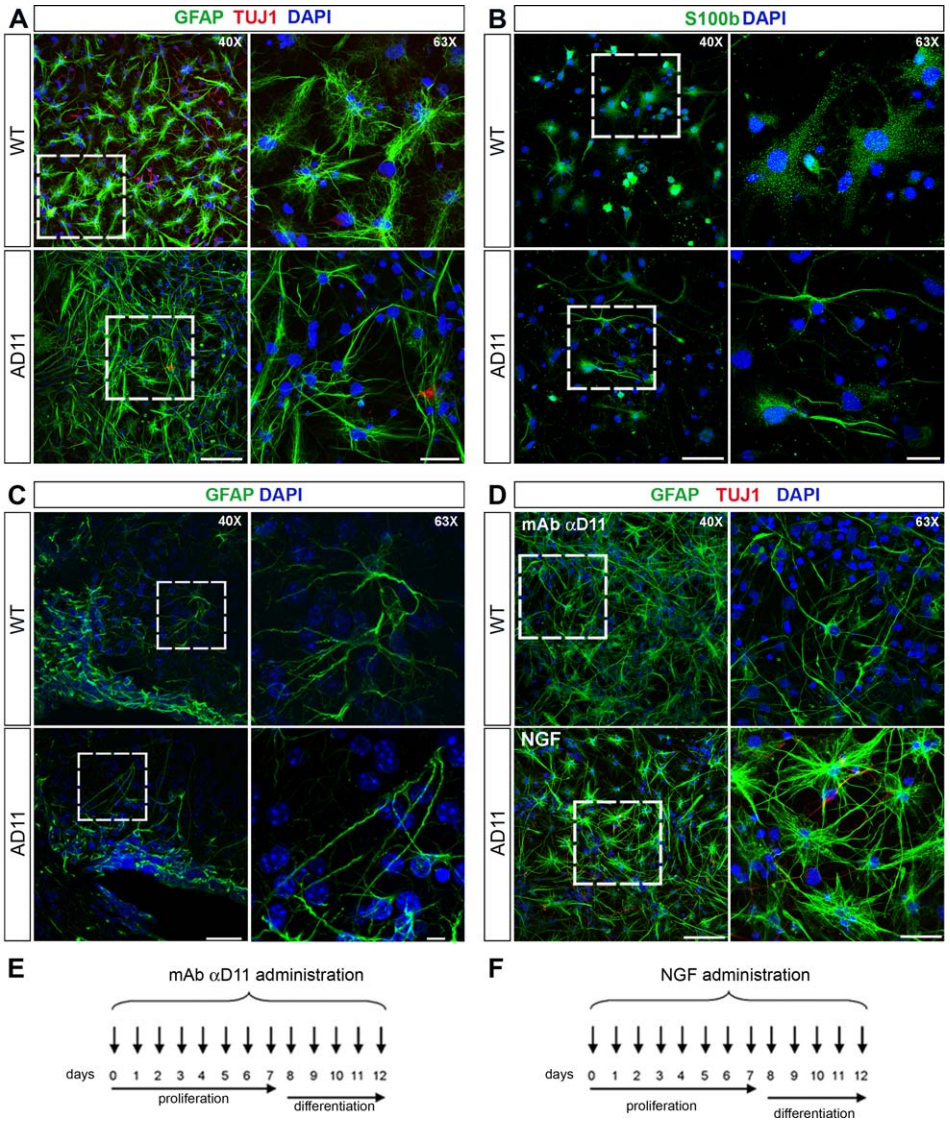

Figure 6. Impaired differentiation of AD11-NSCs. **(A):** Immunofluorescence staining for neurons (TuJ1+, red) and glial cells (GFAP+, green) shows reduced neuronal and glial differentiation of AD11 neurospheres compared to WT. (A, **B**): AD11 astrocytes (GFAP+ and S100b+ cells) display an altered elongated shape, compared to WT counterpart. This phenotype is also present in vivo **(C)**, as shown by GFAP immunostaining (green) in AD11 (bottom) and WT (upper) SVZ regions, which reveals the same morphological defect of NSCs-derived astrocytes. **(D):** Astrocytes defect depends on NGF neutralization. Differentiated cells stained for GFAP (green) from a WT clone treated with 100 ng/ml of mAb anti-NGF (mAb αD11, upper panels) 5 days prior to and 5 days during differentiation (see timeline in **(E)**) show morphological alteration. NGF rescues the astrocytes defects of AD11 progenitors (lower panels). NGF treatment of AD11 progenitors prior and during differentiation (see timeline in **(F)**), partly rescues their astrocytes atrophy, as revealed by GFAP immunostaining (green). (E, F): Timelines of the experiments described in (D). Right panels represent a two zoom magnification (×63) of the insets in the corresponding left panels. Scale bars = 75 and 25 μm (enlargements) in (A, B, and D); 50 and 10 μm (enlargements) in (C). Abbreviations: DAPI, 4,6-diamidine-2-phenylindole dihydrochloride; GFAP, glial fibrillary acid protein; NGF, nerve growth factor; WT, wild type.

astrocytes assume the same elongated shape observed in the cells differentiated from AD11 neurospheres (Fig. 6D, upper panels). Conversely, when we added NGF to AD11 progenitors, during proliferation and differentiation, we could rescue to some extent the glial morphology defects (Fig. 6D, lower panels), and their number increased to approximately 50% (not shown). Both treatments (mAb αD11 on WT cell or NGF on AD11 cells) were effective only when performed both during proliferation and differentiation, whereas had little to none effect when applied after differentiation has begun (Supporting Information Fig. 5), suggesting that functional NGF signaling is required for astrocytes precursors proliferation and differentiation. Indeed, the morphological alteration was already present in immature AD11 astrocytes, identified by the concomitant expression of nestin and GFAP [35], as shown in Figure 7A. Moreover, since AD11 astrocytes also express late differentiation markers such as GFAP and S100b (Figs. 6A, 6B, 7A), we believe that their alteration is not due an inability to terminally differentiate, but most likely to intrinsic cell shaping defects due to cytoskeleton disassembly, as suggested by the drastic reduction in both the acetylated and tyrosinated forms of tubulin (Fig. 7B).

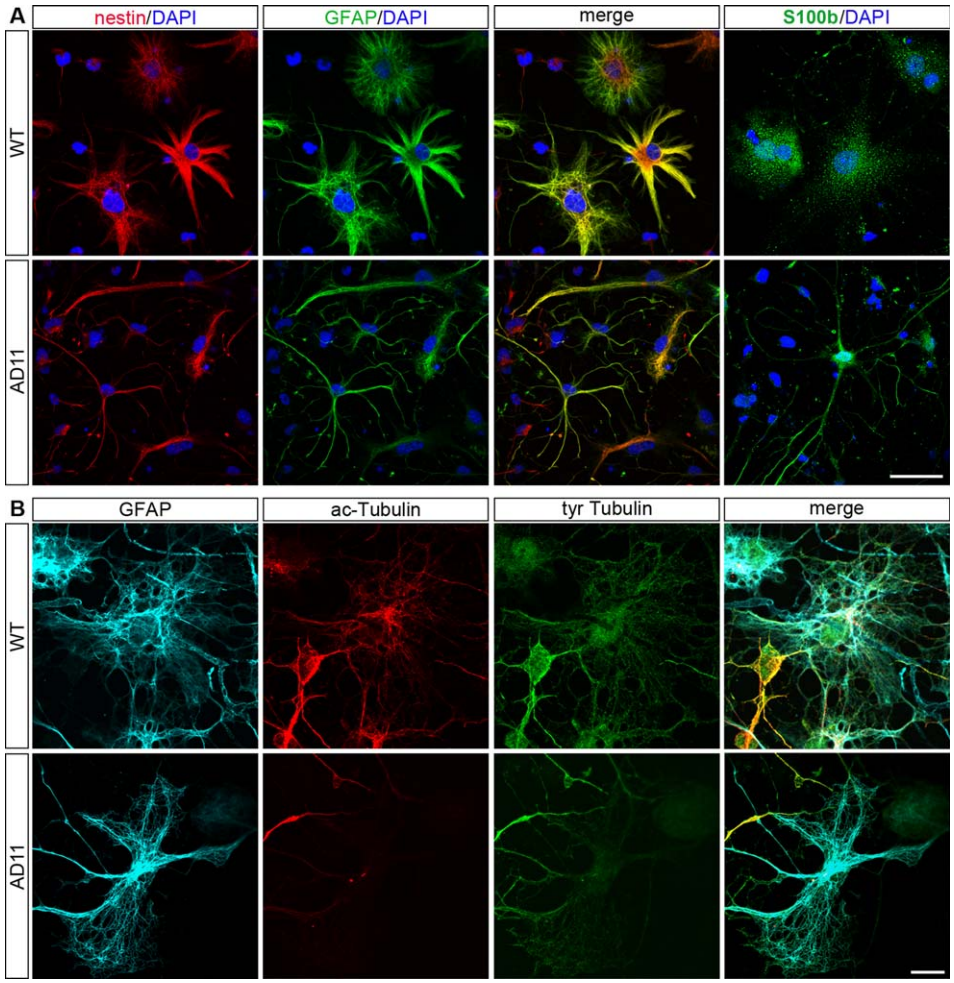

Figure 7. Morphological defects of AD11 astrocytes. **(A):** Morphological alteration of AD11 astrocytes are present both at immature and mature stage of differentiation. Co-expression of nestin (red) and GFAP (green) shows that the morphological defect is already present at more immature stage (nestin+GFAP) in AD11 astrocytes (lower panels) and persists in more mature, S100b expressing astrocytes (right lower panel, green), compared to WT astrocytes (upper panels). **(B):** Immunostaining for acetylated (red) and tyrosinated tubulin (green) shows the drastic reduction of both forms of tubulin in AD11 GFAP+ (cyano) astrocytes (lower panels), compared to WT (upper panels). Scale bars = 50 μm (×63 magnification, zoom 2) in (A), 10 μm in (B) (×63 magnification, zoom 4). Abbreviations: DAPI, 4,6-diamidine-2-phenylindole dihydrochloride; GFAP, glial fibrillary acidic protein; WT, wild type.

Discussion

Here we report for the first time that NGF regulates SVZ neurogenesis, by controlling progenitors' proliferation, neuronal differentiation, and OB newborn neurons' formation. In AD11 mice, NGF neutralization reduces the proliferation of adult SVZ progenitors and therefore the generation of newborn olfactory neurons of approximately 50%, which correlates with an impaired olfaction ability. This phenotype could be responsible for additional neuronal defects in the olfactory nervous system, leading to the formation of a disorganized olfactory epithelium, enlarged in thickness that was previously observed in adult AD11 mice (S. Capsoni, personal communication). Interestingly, these animals fail to discriminate between different odors. However, we cannot exclude that this olfactory discrimination deficit could also depend on other neurogenic defects, such as migration failure along the rostral migratory stream of the AD11 neuroblasts, which needs further investigations.

The proliferative impairment of AD11-NSCs can be reproduced in vitro by acutely treating WT NSCs with the anti-NGF antibody, whereas the addition of exogenous NGF partly rescues AD11 progenitor proliferation, both in vitro and in vivo. These data demonstrate that this AD11 phenotype depends on NGF neutralization occurring in the SVZ progenitors. While NGF expression in the adult SVZ niche has so far been reported only in rats and monkeys [36–38], here we report that NGF is expressed in the mouse SVZ region and in SVZ progenitors at different stages of maturation. This heterogeneity of NGF expression in cell subpopulations of the adult SVZ populations, together with the differential expression of its receptors TrkA and p75 [39], adds complexity to the possible role of NGF in regulating adult NSCs and to the interpretation of the AD11 phenotype. Our data firmly demonstrate that NGF is required both for progenitors' proliferation and differentiation, but we can postulate that it might play a role also in cell fate specification, as demonstrated for the embryonic precursor cells [10]. A more precise mapping of NGF and

NTRs coexpression in the different SVZ populations (i.e., in NGF-GFP transgenic mice, [40]) would help to achieve a better comprehension of the role of this neurotrophic factor in regulating the homeostasis of adult NSCs during the various stages of their development. In addition to the reduced proliferation, we also observed a general alteration in the differentiation potential of AD11 NSCs. While the overall percentage of neurons and astrocytes (βtubulin+ and GFAP+) decreased in AD11 (13% vs. 32% in WT), O4+ oligodendrocytes were more abundant in AD differentiated cultures (2.8 % vs. 0.9% in WT). This latter result suggests that NGF inhibits oligodendrogenesis, similarly to what has been recently reported for proNGF [41].

We also found a severe morphological alteration of AD11 astrocytes, as shown by the atypical elongated shape of GFAP+ cells present both in vitro in the differentiating AD11 neurospheres and in vivo in the SVZ. Since AD11 astrocytes do express markers of mature differentiation, such as GFAP and S100b, we concluded that their morphological defect is not due to an inability of AD11 progenitors to terminally differentiate into astrocytes, but it is rather due to defects in cell shaping (already present at early phase of astrocytic maturation), as demonstrated by the drastic reduction of both the acetylated and tyrosinated forms of tubulin, which suggests a general cytoskeleton disorganization.

The AD11 astrocytes phenotype is reminiscent of similar morphological alterations reported in the glial compartment of animal models for Alzheimer's Disease (AD) [42, 43], that have been associated either to astrocytes atrophy or to astrogliosis observed in different phases of the AD neurodegenerative process [44, 45]. Our results could highlight a role for a proper NGF signaling in maintaining the homeostasis of the glial compartment. Interestingly, when we add mAb αD11 NGF-neutralizing antibody to WT differentiating neurospheres, GFAP+ cells assume the same elongated shape observed in the AD11 ones, demonstrating that this phenotype is due to an acute persistent neutralization of NGF activity in vitro, that mimics the chronic depletion occurring in AD11 mice. Notably, AD11 animals represent a comprehensive murine model for AD-like neurodegeneration, as they progressively develop functional and behavioral impairments that encompass several features of human AD [26, 46]. Indeed, we also demonstrated that AD11 mice have an impaired olfaction ability, which is one of the earliest clinical hallmarks in human AD [47]. Thus, AD11 mice offer the unique opportunity to study adult neurogenesis in a model of neurodegeneration that is NGF-mediated and thus provide the proper molecular and cellular environment in which cross-interactions between an altered NGF signaling and impaired adult neurogenesis can be studied, in connection with the onset of AD neurodegeneration phenotype. So far, changes in the expression levels of NGF and its receptors TrkA and p75 have been reported in different AD mouse models of neurodegeneration [48–50] but never in relationship with possible alterations of adult neurogenesis. In this view, our data not only provide a direct demonstration that NGF regulates the proliferation and differentiation of adult SVZ NSCs but also shed new light on the possible relationships between altered NGF signaling and impaired neurogenesis and gliogenesis observed in AD.

Conclusion

In summary, this article demonstrates that the chronic depletion of NGF occurring in anti-NGF transgenic AD11 mice leads to a severe proliferative and differentiative impairment of SVZ progenitors, both in vivo and in vitro. As a consequence of these defects, AD11 mice have a lower number of newborn neurons in the OB, which correlates with a reduced ability in odor discrimination in these mice. In addition to the neurogenic defect, AD11 progenitors fail also to differentiate properly in glial cells in vitro. Moreover, both SVZ-resident and neurospheres-derived astrocytes display an atrophic morphology. Both this phenotype and the proliferative impairment of AD11 progenitors can be rescued in vitro by NGF treatment. Altogether, our data demonstrate for the first time a direct involvement of NGF in regulating the proliferation of adult NSCs and their differentiation ability.

Acknowledgments

We thank Dr. Francesca Paoletti and Dr. Francesca Malerba for recombinant NGF purification, Dr. Gianluca Amato for mAb αD11 antibody purification and Dr. Andrea Storti for technical help with qReal-time PCR experiments. This work was funded by the Italian Ministry of Higher Education and Scientific Research (FIRB n. RBAP10L8TY), and by Fondazione Roma.

Disclosure of potential conflicts of interest

The authors indicate no potential conflicts of interests.

AUTHOR CONTRIBUTIONS

R.S. and P.C.: conception and design, collection and/or assembly of data, data analysis and interpretation, and manuscript writing; D.V.: collection and/or assembly of data; R.B., M.C., E.P., S. Cintoli, and S. Capsoni: collection and/or assembly of data and data analysis and interpretation; N.B.: conception and design and data analysis and interpretation; A.C.: conception and design, data analysis and interpretation, manuscript writing, and final approval of manuscript. R.S. and P.C. contributed equally to this article.

References

1 Conti L, Pollard SM, Gorba T et al. Niche-independent symmetrical self-renewal of a mammalian tissue stem cell. PLoS Biol 2005;3:e283.

2 Chojnacki AK, Mak GK, Weiss S. Identity crisis for adult periventricular neural stem cells: Subventricular zone astrocytes, ependymal cells or both? Nat Rev Neurosci 2009;10:153–163.

3 Brustle O, McKay RD. Neuronal progenitors as tools for cell replacement in the nervous system. Curr Opin Neurobiol 1996;6:688–695.

4 Zhao C, Deng W, Gage FH. Mechanisms and functional implications of adult neurogenesis. Cell 2008;132:645–660.

5 Ming GL, Song H. Adult neurogenesis in the mammalian brain: Significant answers and significant questions. Neuron 2011;70:687–702.

6 Bibel M, Barde YA. Neurotrophins: Key regulators of cell fate and cell shape in the vertebrate nervous system. Genes Dev 2000; 14:2919–2937.

7 Young KM, Merson TD, Sotthibundhu A et al. p75 neurotrophin receptor expression defines a population of BDNF-responsive neurogenic precursor cells. J Neurosci 2007; 27:5146–5155.

8 Davies AM. Regulation of neuronal survival and death by extracellular signals during development. Embo J 2003;22:2537–2545.

9 Cattaneo E, McKay R. Proliferation and differentiation of neuronal stem cells regulated by nerve growth factor. Nature 1990; 347:762–765.

10 Lachyankar MB, Condon PJ, Quesenberry PJ et al. Embryonic precursor cells that express Trk receptors: Induction of different cell fates by NGF, BDNF, NT-3, and CNTF. Exp Neurol 1997;144:350–360.

11 Nakajima M, Ishimuro T, Kato K et al. Combinatorial protein display for the cell-based screening of biomaterials that direct neural stem cell differentiation. Biomaterials 2007;28:1048–1060.

12 Moscatelli I, Pierantozzi E, Camaioni A et al. p75 neurotrophin receptor is involved in proliferation of undifferentiated mouse embryonic stem cells. Exp Cell Res 2009;315: 3220–3232.

13 Lee TH, Kato H, Chen ST et al. Expression of nerve growth factor and trkA after transient focal cerebral ischemia in rats. Stroke 1998;29:1687–1696; discussion 1697.

14 Zhu W, Cheng S, Xu G et al. Intranasal nerve growth factor enhances striatal neurogenesis in adult rats with focal cerebral ischemia. Drug Deliv 2011;18:338–343.

15 Galvao RP, Garcia-Verdugo JM, Alvarez-Buylla A. Brain-derived neurotrophic factor signaling does not stimulate subventricular zone neurogenesis in adult mice and rats. J Neurosci 2008;28:13368–13383.

16 Gascon E, Vutskits L, Zhang H et al. Sequential activation of p75 and TrkB is involved in dendritic development of subventricular zone-derived neuronal progenitors in vitro. Eur J Neurosci 2005;21:69–80.

17 Ruberti F, Capsoni S, Comparini A et al. Phenotypic knockout of nerve growth factor in adult transgenic mice reveals severe deficits in basal forebrain cholinergic neurons, cell death in the spleen, and skeletal muscle dystrophy. J Neurosci 2000;20:2589–2601.

18 Paoletti F, Covaceuszach S, Konarev PV et al. Intrinsic structural disorder of mouse proNGF. Proteins 2009;75:990–1009.

19 Capsoni S, Giannotta S, Cattaneo A. Nerve growth factor and galantamine ameliorate early signs of neurodegeneration in anti-nerve growth factor mice. Proc Natl Acad Sci USA 2002;99:12432–12437.

20 Gritti A, Galli R, Vescovi AL. Cultures of stem cells of the central nervous system. Protoc Neural Cell Cult 2001:173-0000.

21 Gritti A, Galli R, Vescovi AL. Clonal analyses and cryopreservation of neural stem cell cultures. Methods Mol Biol 2008;438:173–184.

22 Cattaneo A, Rapposelli B, Calissano P. Three distinct types of monoclonal antibodies after long-term immunization of rats with mouse nerve growth factor. J Neurochem 1988;50:1003–1010.

23 Ceci M, Welshhans K, Ciotti MT et al. RACK1 is a ribosome scaffold protein for beta-actin mRNA/ZBP1 complex. PLoS One 2012;7:e35034.

24 Livak KJ, Schmittgen TD. Analysis of relative gene expression data using real-time quantitative PCR and the 2(-Delta Delta C(T)) Method. Methods 2001;25:402–408.

25 Galli R, Fiocco R, De Filippis L et al. Emx2 regulates the proliferation of stem cells of the adult mammalian central nervous system. Development 2002;129:1633–1644.

26 Capsoni S, Ugolini G, Comparini A et al. Alzheimer-like neurodegeneration in aged antinerve growth factor transgenic mice. Proc Natl Acad Sci USA 2000;97:6826–6831.

27 Capsoni S, Ruberti F, Di Daniel E et al. Muscular dystrophy in adult and aged anti-NGF transgenic mice resembles an inclusion body myopathy. J Neurosci Res 2000;59:553–560.

28 D'Onofrio M, Arisi I, Brandi R et al. Early inflammation and immune response mRNAs in the brain of AD11 anti-NGF mice. Neurobiol Aging 32:1007–1022.

29 De Rosa R, Garcia AA, Braschi C et al. Intranasal administration of nerve growth factor (NGF) rescues recognition memory deficits in AD11 anti-NGF transgenic mice. Proc Natl Acad Sci USA 2005;102:3811–3816.

30 Fuentealba LC, Obernier K, Alvarez-Buylla A. Adult neural stem cells bridge their niche. Cell Stem Cell 2012;10:698–708.

31 Imayoshi I, Sakamoto M, Ohtsuka T et al. Roles of continuous neurogenesis in the structural and functional integrity of the adult forebrain. Nat Neurosci 2008;11:1153–1161.

32 Clark RE, Broadbent NJ, Zola SM et al. Anterograde amnesia and temporally graded retrograde amnesia for a nonspatial memory task after lesions of hippocampus and subiculum. J Neurosci 2002;22:4663–4669.

33 Ryan BC, Young NB, Moy SS et al. Olfactory cues are sufficient to elicit social approach behaviors but not social transmission of food preference in C57BL/6J mice. Behav Brain Res 2008;193:235–242.

34 Bertrand N, Castro DS, Guillemot F. Proneural genes and the specification of neural cell types. Nat Rev Neurosci 2002;3:517–530.

35 Sergent-Tanguy S, Michel DC, Neveu I et al. Long-lasting coexpression of nestin and glial fibrillary acidic protein in primary cultures of astroglial cells with a major participation of nestin(+)/GFAP(−) cells in cell proliferation. J Neurosci Res 2006;83:1515–1524.

36 Tonchev AB. Brain ischemia, neurogenesis, and neurotrophic receptor expression in primates. Arch Ital Biol 2011;149:225–231.

37 Tonchev AB, Yamashima T, Guo J et al. Expression of angiogenic and neurotrophic factors in the progenitor cell niche of adult monkey subventricular zone. Neuroscience 2007;144:1425–1435.

38 Triaca V, Tirassa P, Aloe L. Presence of nerve growth factor and TrkA expression in the SVZ of EAE rats: Evidence for a possible functional significance. Exp Neurol 2005;191: 53–64.

39 Takahashi J, Palmer TD, Gage FH. Retinoic acid and neurotrophins collaborate to regulate neurogenesis in adult-derived neural stem cell cultures. J Neurobiol 1999;38:65–81.

40 Kawaja MD, Smithson LJ, Elliott J et al. Nerve growth factor promoter activity revealed in mice expressing enhanced green fluorescent protein. J Comp Neurol 2011;519: 2522–2545.

41 Guo J, Wang J, Liang C et al. proNGF inhibits proliferation and oligodendrogenesis of postnatal hippocampal neural stem/progenitor cells through p75NTR in vitro. Stem Cell Res 2013;11:874–887.

42 Rodriguez JJ, Jones VC, Tabuchi M et al. Impaired adult neurogenesis in the dentate gyrus of a triple transgenic mouse model of Alzheimer's disease. PLoS One 2008;3:e2935.

43 Rodriguez JJ, Olabarria M, Chvatal A et al. Astroglia in dementia and Alzheimer's disease. Cell Death Differ 2009;16:378–385.

44 Verkhratsky A, Olabarria M, Noristani HN et al. Astrocytes in Alzheimer's disease. Neurotherapeutics 2010;7:399–412.

45 Olabarria M, Noristani HN, Verkhratsky A et al. Concomitant astroglial atrophy and astrogliosis in a triple transgenic animal model of Alzheimer's disease. Glia 2010;58: 831–838.

46 Capsoni S, Brandi R, Arisi I et al. A dual mechanism linking NGF/proNGF imbalance and early inflammation to Alzheimer's disease neurodegeneration in the AD11 anti-NGF mouse model. CNS Neurol Disord Drug Targets 2011;10:635–647.

47 Djordjevic J, Jones-Gotman M, De Sousa K et al. Olfaction in patients with mild cognitive impairment and Alzheimer's disease. Neurobiol Aging 2008;29:693–706.

48 Schulte-Herbruggen O, Eckart S, Deicke U et al. Age-dependent time course of cerebral brain-derived neurotrophic factor, nerve growth factor, and neurotrophin-3 in APP23 transgenic mice. J Neurosci Res 2008;86: 2774–2783.

49 Jaffar S, Counts SE, Ma SY et al. Neuropathology of mice carrying mutant APP(swe) and/or PS1(M146L) transgenes: alterations in the p75(NTR) cholinergic basal forebrain septohippocampal pathway. Exp Neurol 2001; 170:227–243.

50 Perez SE, He B, Muhammad N et al. Cholinotrophic basal forebrain system alterations in 3xTg-AD transgenic mice. Neurobiol Dis 2011;41:338–352.

See www.StemCells.com for supporting information available online.